Journal of Solution Chemistry (2021) 50:443–457
https://doi.org/10.1007/s10953-021-01080-9

Solubility of PuO_2(am,hyd) and the Formation of Pu(IV) Carbonate Complexes in Carbonate Solutions Containing 0.1–5.0 mol·dm^{-3} $NaNO_3$

Taishi Kobayashi[1] · **David Fellhauer**[2] · **Takayuki Sasaki**[1]

Received: 17 July 2020 / Accepted: 22 March 2021 / Published online: 15 April 2021
© The Author(s), under exclusive licence to Springer Science+Business Media, LLC, part of Springer Nature 2021

Abstract
The solubility of plutonium hydrous oxide (PuO_2(am, hyd)) was investigated in the presence of carbonate in neutral to alkaline, dilute to concentrated sodium nitrate ($NaNO_3$) solutions. The observed dependence of the Pu(IV) solubility in low to medium concentration $NaNO_3$ agreed with previously reported data and was well reproduced by the thermodynamic model curves, containing the species $Pu(CO_3)_4^{4-}$, $Pu(CO_3)_5^{6-}$, and $Pu(OH)_2(CO_3)_2^{2-}$. Significant deviations between experimental and modeled Pu(IV) solubility were, however, observed for 2 mol·dm^{-3} $NaNO_3$ solutions. A more comprehensive chemical model including the complex $Pu(OH)_2(CO_3)_3^{4-}$ was established, that reproduces the experimental results reasonably well. The conditional complex formation constants for $Pu(OH)_2(CO_3)_3^{4-}$ were extrapolated to $I=0$ using the specific ion interaction theory (SIT) and Pitzer approaches, and the corresponding ion interaction parameters were evaluated.

Keywords Solubility · PuO_2(am,hyd) · Carbonate · Complex formation · Ionic strength

1 Introduction

Safety assessment of radioactive waste management requires the prediction of the solubility limit of radionuclides under relevant repository conditions. Under the geochemical conditions of radioactive waste disposal, tetravalent plutonium (Pu(IV)) is only sparingly soluble and forms oxy-hydroxide or hydrous oxide solid phases, described as $Pu(OH)_4$(am), $PuO_2{\cdot}xH_2O$(s), or PuO_2(am,hyd), etc. [1–6]. Plutonium(IV) solubility in the absence of complexing ligands has been investigated in a number of literature studies indicating a value in the range of 10^{-10} to 10^{-8} mol·dm^{-3} [7–10] under neutral to alkaline pH conditions. On the other hand, carbonate ion (CO_3^{2-}), a relevant ligand in repository systems, is known to form strong complexes with Pu(IV) [7, 9]. The formation of Pu(IV) carbonate

✉ Taishi Kobayashi
kobayashi@nucleng.kyoto-u.ac.jp

[1] Department of Nuclear Engineering, Graduate School of Engineering, Kyoto University, Kyotodaigaku-katura, Nishikyo, Kyoto 615-8540, Japan

[2] Institute for Nuclear Waste Disposal, Karlsruhe Institute of Technology, P.O. Box 3640, 76021 Karlsruhe, Germany

complexes potentially enhances the apparent solubility of Pu(IV) oxy-hydroxide or hydrous oxide solid phases. A robust thermodynamic model for the complexation of Pu(IV) with carbonate based on the thermodynamic constant, is therefore required for a reliable prediction of the migration behavior of plutonium.

The complexation of Pu(IV) carbonate has been investigated in several studies [11–15]. Capdevila et al. measured UV–Vis spectra of Pu(IV) in (0.1 to 1.5) mol·dm^{-3} sodium carbonate (Na_2CO_3) solutions and suggested the existence of $Pu(CO_3)_4^{4-}$ and $Pu(CO_3)_5^{6-}$ based on the molar absorbance of the Pu(IV) solutions as a function of CO_3^{2-} concentration [12]. The ionic strength (I) controlled by the Na_2CO_3 concentration was corrected by the specific ion interaction theory (SIT) [9] and the stepwise complexation constant (K_5) from $Pu(CO_3)_4^{4-}$ to $Pu(CO_3)_5^{6-}$ was calculated to be $\log_{10} K_5^o = -1.36 \pm 0.09$ [12]. The formation of $Pu(CO_3)_5^{6-}$ under high carbonate concentration was further confirmed by structural analysis with extended X-ray absorption fine structure (EXAFS) spectroscopy [13]. Rai et al. conducted solubility measurements of PuO_2(am) in K_2CO_3 solutions ranging in concentration from 0.1 to 6.2 mol·kg^{-1}. The dependence of Pu(IV) solubility on carbonate concentration at $[CO_3^{2-}] > 1$ mol·kg^{-1} also indicated the formation of $Pu(CO_3)_5^{6-}$ as the dominant solution species [14]. The ionic strength of the Pu(IV) solutions where $Pu(CO_3)_5^{6-}$ is dominant was rather large due to high CO_3^{2-} concentration, and the Pitzer approach [16, 17] was used to correct for ionic strength effects [14]. The formation constant of $Pu(CO_3)_5^{6-}$ (β_{105}) was determined to be $\log_{10} \beta_{105}^o = 34.18$ when combined with the solubility product of PuO_2(am) ($\log_{10} K_{sp}^o = -56.85$ [18]). These studies have been comprehensively reviewed and recommended formation constants for $Pu(CO_3)_4^{4-}$ and $Pu(CO_3)_5^{6-}$ were selected to be $\log_{10} \beta_{104}^o = 37.0 \pm 1.1$ and $\log_{10} \beta_{105}^o = 35.65 \pm 1.13$ as part of the Nuclear Energy Agency Thermochemical Database Project (NEA-TDB) [7, 9].

The Pu(IV) carbonate system at lower CO_3^{2-} concentrations ($[CO_3^{2-}] < 0.1$ mol·kg^{-1}) has been investigated in [11, 14], and [15]. Yamaguchi et al. measured the solubility of $PuO_2{\cdot}xH_2O$(s) in the presence of (10^{-4} to 0.1) mol·dm^{-3} total carbonate at constant ionic strength of $I = 0.1$ mol·dm^{-3} [11]. According to the Pu(IV) solubility dependences on CO_3^{2-} concentration, the authors claimed that neither $Pu(CO_3)_4^{4-}$ nor $Pu(CO_3)_5^{6-}$ could reproduce their experimental data and suggested the formation of ternary $Pu(OH)_2(CO_3)_2^{2-}$ at pH 9.4–10.1 and $Pu(OH)_4(CO_3)_2^{4-}$ at pH 12–13, respectively [11]. The ternary species of $Pu(OH)_2(CO_3)_2^{2-}$ was also proposed by Rai et al. as the predominant Pu(IV) species to explain the Pu(IV) solubility behavior in pH-neutral 0.01 to 1.0 mol·kg^{-1} $KHCO_3$ solutions [14]. The formation constant determined after ionic strength correction by Pitzer approach was $\log_{10} \beta_{122}^o = 44.76$ in combination with $\log_{10} K_{sp}^o = -56.85$ [18]. On the other hand, Schepperle et al. have recently investigated the solubility of PuO_2(am,hyd) in the presence of 0.1 and 0.04 mol·dm^{-3} Na_2CO_3/$NaHCO_3$ at pH 8–12.5 and $I = 0.1$–5.0 mol·dm^{-3} NaCl, and of UO_2(am,hyd) and NpO_2(am,hyd) under analogous solution conditions [15]. It was found that the ternary carbonate complexes of $An(IV)(OH)_2(CO_3)_3^{4-}$ (An(IV) = Pu(IV), U(IV), and Np(IV)) well reproduced the systematic trend of the solubility data as a function of carbonate concentration and pH [15].

In the context of geological disposal of radioactive waste from a reprocessing plant (TRU waste), radionuclides will come in contact with solutions with a wide range of sodium nitrate ($NaNO_3$) concentrations [19–21]. On the other hand, calcium ions leached from the cementitious materials in a repository may limit the CO_3^{2-} concentration due to the precipitation of $CaCO_3$(s) [20, 22]. For the safety assessment of the geological disposal under possible scenarios, a comprehensive thermodynamic model covering various pH, carbonate, and ionic strength conditions are needed. As outlined above, reported data on the Pu(IV) carbonate complex formation are still limited, especially under low CO_3^{2-} concentrations. The

present study focuses on the Pu(IV)–carbonate interaction at low CO_3^{2-} concentration ($[CO_3^{2-}] < 0.3$ mol·dm^{-3}) in dilute to concentrated $NaNO_3$ solutions. The solubility was investigated across a range of hydrogen ion concentrations (pH_c) values of pH_c 8–11, carbonate concentrations of $[CO_3^{2-}] = 10^{-3} - 0.3$ mol·dm^{-3}, and ionic strengths of $I = 0.1 - 5.0$ mol·dm^{-3} ($NaNO_3$). Comprehensive thermodynamic evaluation of the experimental solubility behavior revealed the predominance of soluble Pu(IV) complexes, as summarized in Sect. 3.2.1. The corresponding formation constants were determined by least-squares fitting analyses of the solubility data. The obtained formation constants at different ionic strengths were corrected by the SIT and Pitzer approaches, and the ion interaction parameters determined and compared within the actinide(IV) series.

2 Experimental Section

2.1 Chemicals Used

All chemicals used were of reagent grade. $NaNO_3$ (> 99.0%), $NaNO_2$ (> 98.5%), $NaHCO_3$ (> 99.5%), $Na_2S_2O_4$ (> 80.0%), $NH_2OH{\cdot}HCl$ (> 99.0%), HNO_3 (60 − 61%), and NaOH (> 97.0%) were purchased from Wako Pure Chem. and used without no further purification. Deionized purified water (Milli-Q, Millipore) was used in all solution preparations. All experiments were performed at 25 ± 2 °C.

2.2 Analytical Methods

A combination glass electrode (9615-10D, Horiba Ltd.) was used to measure the pH_c. The filling solution of the electrode was composed of aqueous sodium chloride (NaCl, 3.6 mol·dm^{-3}) and sodium perchlorate ($NaClO_4$, 0.4 mol·dm^{-3}) (> 98.0%, Wako Pure Chem.). Since the experimentally measured pH values (pH_{exp}) depend on the ionic strength of solutions, the electrode was calibrated against standard HNO_3 and NaOH solutions (pH_c 1, 2, 3, 11, 12, and 13; > 99.0%, Wako Pure Chem.) at ionic strengths I = (0.1, 0.5, 2.0, and 5.0) mol·dm^{-3} prepared by using appropriate amount of $NaNO_3$. The pH_{exp} values were corrected to the pH_c values at the respective ionic strength. The "A" and "B" values in the equation of $pH_c = A \times pH_{exp} + B$ were determined to be 1.08 and − 0.88 (I = 0.1 mol·dm^{-3}), 1.04 and − 0.20 (I = 0.5 mol·dm^{-3}), 1.06 and − 0.22 (I = 2.0 mol·dm^{-3}), and 1.08 and − 0.47 (I = 5.0 mol·dm^{-3}).

The redox potentials in solution were determined with a Pt combination electrode (9300-10D, Horiba Ltd.) equipped with a Ag/AgCl reference system. The measured redox potential value was taken after several minutes and converted into Eh (redox potential vs. standard hydrogen electrode) by addition of the Ag/AgCl reference electrode potential (+ 208 mV for 3 mol·dm^{-3} KCl junction electrolyte). The apparent electron activity ($pe = -\log a_{e^-}$) was calculated from $Eh = -(RT/F) \ln a_{e^-}$ according to the relation $pe = 16.9$ Eh (V) at 25 °C. The error in the pH_c and Eh values were estimated to be ± 0.05 and ± 20 mV (about 0.3 pe units) from the reading values.

2.3 Solubility Experiment

2.3.1 Purification of Plutonium

The plutonium (^{239}Pu) acidic solution of approximately 10^{-4} mol·dm^{-3} was purified by the following manner. An aliquot of 0.5 mol·dm^{-3} $FeCl_3$ (> 98.0%, Wako Pure Chem.) solution was added to the Pu solution resulting in $[Fe^{3+}] = 0.05$ mol·dm^{-3}. NaOH solution was added to neutralize the solution and precipitate $Fe(OH)_3$(s). Plutonium co-precipitated with $Fe(OH)_3$(s) was washed with purified water several times and then dissolved in 8 mol·dm^{-3} HNO_3. The Pu solution containing dissolved Fe^{3+} in 8 mol·dm^{-3} HNO_3 was purified by anion exchange resin (Dowex 1X8) and subsequently eluted with a 0.1 mol·dm^{-3} $HNO_3 + NH_2OH$ solution. An aliquot of 0.1 mol·dm^{-3} $NaNO_2$ solution was added to the purified solution to oxidize Pu to Pu(IV). Figure 1 shows the absorption spectra of the obtained Pu solution, confirming Pu(IV) as the dominant oxidation state. Plutonium concentration of the solution was determined to be 3.0×10^{-3} mol·dm^{-3} by α-spectrometry (SEIKO EG&G. Co. Ltd.). An aliquot of NaOH solution was added to the Pu(IV) solution to neutralize and prepare the stock suspension of Pu(IV) amorphous hydrous oxide (PuO_2(am,hyd)). The Pu concentration of the PuO_2(am,hyd) stock suspension was 3.8×10^{-3} mol·dm^{-3} (dissolved equivalent).

2.3.2 Solubility Measurements

Pu(IV) sample solutions for solubility experiments were prepared by the undersaturation method and stored in an Ar glove box ($O_2 < 100$ ppm) at 25 °C. Aliquots of HNO_3 and/or NaOH, $NaHCO_3$, and $NaNO_3$ solutions were mixed in polypropylene tubes to prepare sample solutions of 8 mL volume with a specific pH_c, total carbonate concentration ($[C]_{tot}$), and ionic strength (I). The pH_c ranged from 8 to 12, and the $[C]_{tot}$ ranged from 0.001 to 0.3 mol·dm^{-3}. The ionic strength was fixed at $I = (0.1, 0.5, 2.0$ or $5.0)$ mol·dm^{-3} within ± 10%; 0.08 mL of 0.1 mol·dm^{-3} $Na_2S_2O_4$ was added to the sample solutions as a reductant to stabilize Pu(IV) during the experiment. A 0.2 mL of PuO_2(am,hyd) stock suspension was then added to the polypropylene tubes, corresponding to a total inventory of ca. 20 μg or $[Pu] = 1.0 \times 10^{-4}$ mol·dm^{-3}, respectively.

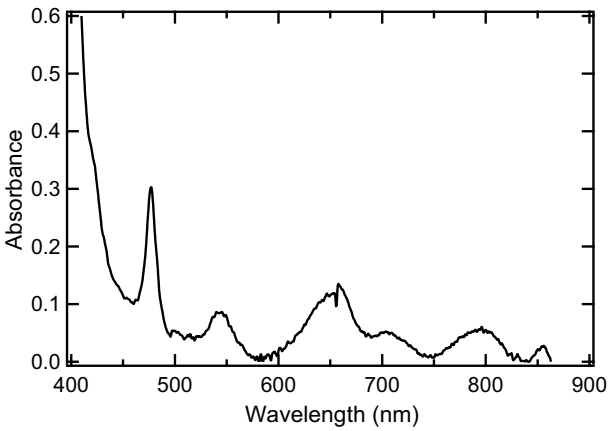

Fig. 1 UV–Vis spectra of the Pu(IV) stock solution

The sample tubes were then equilibrated for up to 43 weeks and occasionally shaken by hand for a few minutes throughout the aging process. After the given aging time, the pH_c and Eh values of each sample solution were measured. An aliquot of 0.2 mL of supernatant of the sample solution was then filtered through ultrafiltration membranes (Microcon NMWL 10 kDa, corresponding to pore sizes of approximately 3 nm, Millipore). After filtration, a 30 µL of concentrated HNO_3 was added to the filtrate immediately to avoid any sorption of Pu species on the filtration tube. 30 µL of the acidified filtrate was dried in a stainless sample pan using an infrared lamp and analyzed at the 5.244 meV alpha line of ^{239}Pu by α-spectrometry. A peak of 5.244 meV with lower-energy side tail, typical for the high ionic strength samples, is possibly caused self-absorption by deposited electrolyte. Measurements of sample solutions with known ^{239}Pu concentration at different electrolyte concentrations were used for the correction of self-absorption effect. The detection limit for total Pu concentration ($[Pu]_{tot}$) corresponded to about 1×10^{-8} mol·dm^{-3}. The standard error for the α-spectrometry calculated from each count was within 5%, which resulted in ±0.05 logarithmic unit of $[Pu]_{tot}$ for most of the samples by taking an appropriate measurement time. The free carbonate ion concentration ($[CO_3^{2-}]$) was calculated from $[C]_{tot}$, measured pH_c values, and the dissociation constants of carbonate and bicarbonate with uncertainties of $\pm10\%$ in $[CO_3^{2-}]$, assuming that the concentrations of Pu carbonate complexes were negligible compared to $[C]_{tot}$. For the thermodynamic analysis of the experimental data, the molar concentration (mol·dm^{-3}) was converted to the molal scale (mol·kg^{-1}) according to the densities of $0.1-5.0$ mol·dm^{-3} $NaNO_3$ solutions.

3 Results and Discussion

3.1 Pu Solubility in the Presence of Carbonate in 0.1 – 5.0 mol·dm^{-3} $NaNO_3$

Figure 2 shows the experimentally measured pH_c ($-\log_{10}[H^+]$) and pe values of the sample solutions after aging for 64–302 days, together with the calculated Pu stability field based on the chemical diagram calculation program [23]. The observed pe values were at around $pe=2.5\pm0.7$ and showed no strong dependence on pH_c 8.5 to 11.5 and $I=0.5$ and 2.0 mol·dm^{-3}. In the neutral to alkaline pH region, Pu(IV) as PuO_2(am,hyd) has a large stability field and all obtained pe values were within the stability field of Pu(IV) [24]. It is noteworthy that the observed pe values were considerably high, although 1 mmol·dm^{-3} $Na_2S_2O_4$ was used to keep a strong reducing condition. Similar observations were reported by Baumann et al. [25]. Whereas, measured pe values in NaCl–$NaNO_3$–NaOH systems in the presence of $Na_2S_2O_4$ were around $pe=-10$ at pH around 12, a significant increase in pe was observed for the same system in the presence of $TcO_2{\cdot}0.6H_2O$(am) [25], likely due to redox reactions between nitrate and Tc(IV). Although $PuO_2{\cdot}xH_2O$(am) is not likely to be reduced or oxidized under the condition of observed pe values according to its redox borderline, an excess amount of $NaNO_3$ may play a role to increase the pe values in the presence of $Na_2S_2O_4$.

In Fig. 3, the Pu solubility in the presence of $[C]_{tot}=0.16$ mol·dm^{-3} in $I=0.5$ and 2.0 mol·dm^{-3} $NaNO_3$ are plotted as a function of pH_c ($-\log_{10}[H^+]$). Compared with the Pu(IV) solubility in the absence of carbonate [1, 14, 26, 27], the obtained solubility values were orders of magnitude higher, indicating the formation of Pu(IV) carbonate complexes. At $I=0.5$ mol·dm^{-3} $NaNO_3$, the solubility around pH_c 9 was between 10^{-6} and 10^{-7} mol·dm^{-3} and decreased with increasing pH_c at $pH_c<10.5$. Since no

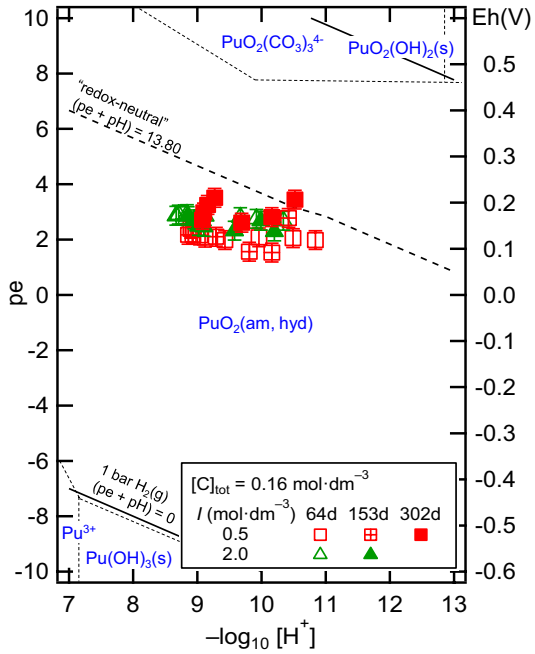

Fig. 2 pH_c and pe values of Pu sample solutions in the presence of $[C]_{tot}=0.16$ mol·dm^{-3} in $I=0.5$ and 2.0 mol·dm^{-3} $NaNO_3$. Pu stability field in the presence of $[C]_{tot}=0.16$ mol·dm^{-3} at $I=0.5$ mol·dm^{-3} $NaNO_3$ with the total Pu concentration ($[Pu]_{tot}$) $=10^{-4}$ mol·dm^{-3} was obtained by the chemical diagram calculation program [23] (Color figure online)

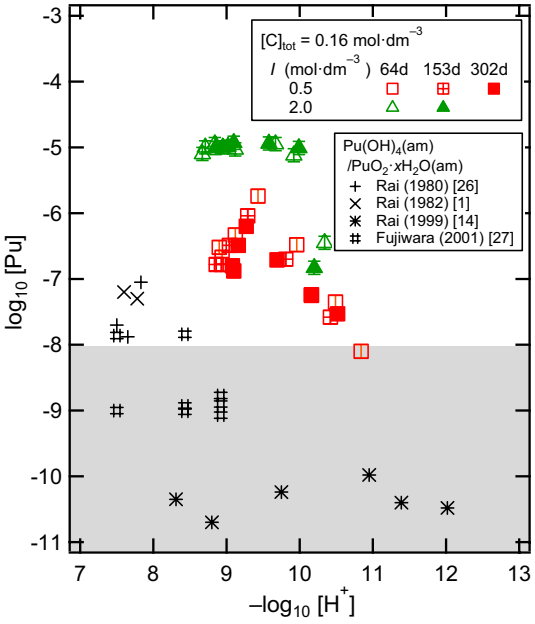

Fig. 3 Pu solubility in the presence of $[C]_{tot}=0.16$ mol·dm^{-3} in $I=0.5$ and 2.0 mol·dm^{-3} $NaNO_3$ as a function of pH_c, together with those in the absence of carbonate [1, 14, 26, 27]. The detection limit of the α-spectrometer used in the present study is indicated by the gray field (Color figure online)

significant difference of the solubility values after aging for 64–302 days was observed, the steady state within the investigated periods has been confirmed after 64 days. At $I=2.0$ mol·dm^{-3} $NaNO_3$, the solubility was more than one order of magnitude higher than that at $I=0.5$ mol·dm^{-3}. A comparable increase of the solubility with increasing

ionic strength was also observed for the Zr(IV)–oxyhydroxide system in the presence of carbonate in $I = 0.1$–5.0 mol·dm^{-3} $NaNO_3$, where Zr was used as an analog of Pu [28].

Figure 4 shows the Pu solubility at pH_c 8.1–9.7 in $I = 0.1 - 5.0$ mol·dm^{-3} $NaNO_3$ as a function of $[C]_{tot}$. The reported solubility data by [11] and [14] were plotted for comparison. The solubility increased systematically with increasing $[C]_{tot}$. Provided that the solid phase was PuO_2(am,hyd), the observed slope ($\log_{10}$ [Pu] vs. $\log_{10}$ $[C]_{tot}$) of 3–4 indicated that 3 or 4 carbonate ions are involved in the complex formation of the predominant Pu(IV) carbonate species [29]. The strong, positive dependence of Pu(IV) solubility on ionic strength is clearly visible from Fig. 4, suggesting the presence of highly charged Pu(IV) complexed species. Solubility values by [14] obtained at pH_c 8.8–9.3 are close to the ones of the present study at $I = 0.1$ mol·dm^{-3} $NaNO_3$ in the range of $[C]_{tot} < 0.1$ mol·dm^{-3}. Considering that the background electrolyte in [14] was pure $KHCO_3$, both data are in good agreement under comparative experimental conditions of pH_c and ionic strength. On the other hand, the solubility values reported by [11] are 1–2 orders of magnitude higher than those determined for $I = 0.1$ mol·dm^{-3} $NaNO_3$ in the present study, in spite of similar pH_c and ionic strength conditions. In their solubility studies, the sample solutions were prepared from oversaturation with a maximum Pu concentration of 1.3×10^{-6} mol·dm^{-3}, whereas experiments in the present study and in [14] were performed from undersaturation using significantly greater total inventory of Pu solid phases. The oversaturation method from low initial concentration might result in the formation of colloidal Pu(IV) oxyhydroxides with higher solubility [30, 31].

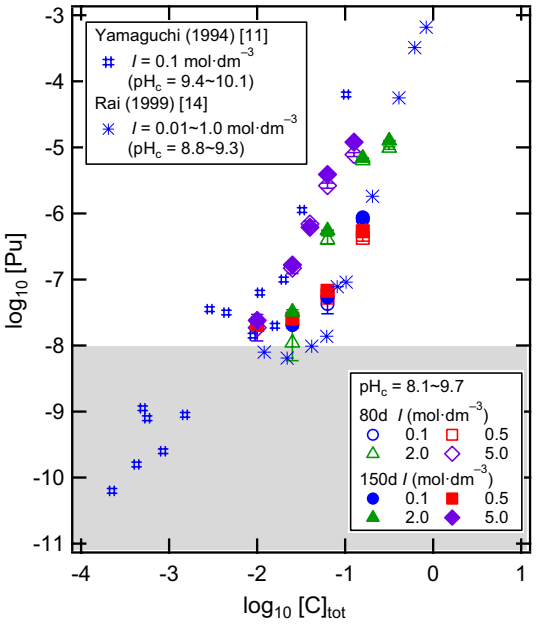

Fig. 4 Pu solubility at pH_c 8.1–9.7 in $I = 0.1 - 5.0$ mol·dm^{-3} $NaNO_3$ as a function of $[C]_{tot}$. The detection limit of the α-spectrometer is indicated by the gray field (Color figure online)

3.2 Thermodynamic Model of Pu Solubility in the Na^+–HCO_3^-–CO_3^{2-}–NO_3^-–H_2O System

3.2.1 Comparison with the Existing Thermodynamic Model

The equilibrium reactions for the dissolution of PuO_2(am,hyd) and the formation of the Pu(IV) carbonate complexes, $Pu(OH)_x(CO_3)_y^{4-x-2y}$, can be described as:

$$PuO_2(am,hyd) + 2H_2O \rightleftharpoons Pu^{4+} + 4OH^- \tag{1}$$

$$K_{sp} = [Pu^{4+}][OH^-]^4 \tag{2}$$

$$Pu^{4+} + xOH^- + yCO_3^{2-} \rightleftharpoons Pu(OH)_x(CO_3)_y^{4-x-2y} \tag{3}$$

$$\beta_{1xy} = [Pu(OH)_x(CO_3)_y^{4-x-2y}] \Big/ [Pu^{4+}][OH^-]^x[CO_3^{2-}]^y \tag{4}$$

where K_{sp} and β_{1xy} represent the conditional solubility product and complex formation constant at a certain ionic strength, respectively. The β_{1xy} value determined from the experimental solubility depends directly on the K_{sp} value used in the analysis. Since the K_{sp} value is subject to the state of solid phase that varies with experimental conditions reported in literature sources, we used the complex formation constant, K_{1xy}, defined as below.

$$PuO_2(am,hyd) + 2H_2O + yCO_3^{2-} \rightleftharpoons Pu(OH)_x(CO_3)_y^{4-x-2y} + (4-x)OH^- \tag{5}$$

$$K_{1xy} = [Pu(OH)_x(CO_3)_y^{4-x-2y}][OH^-]^{4-x} \Big/ [CO_3^{2-}]^y \tag{6}$$

In the literature on the Pu(IV) carbonate complexes [11–15], binary complexes of $Pu(CO_3)_4^{4-}$ and $Pu(CO_3)_5^{6-}$ [12–14], and ternary complexes of $Pu(OH)_2(CO_3)_2^{2-}$ [11, 14], $Pu(OH)_4(CO_3)_2^{4-}$ [11] and $Pu(OH)_2(CO_3)_3^{4-}$ [15] have been suggested depending on the experimental conditions. The complex formation constants (K_{1xy}) of $Pu(CO_3)_4^{4-}$, $Pu(CO_3)_5^{6-}$, and $Pu(OH)_2(CO_3)_2^{2-}$ reported in the literature are in relatively good agreement as shown in Table 1. The Pu solubility ($[Pu]_{tot}$) can be calculated as a sum of the concentrations of these species based on their reported complex formation constants.

$$\begin{aligned}[Pu]_{tot} &= [Pu(CO_3)_4^{4-}] + [Pu(CO_3)_5^{6-}] + [Pu(OH)_2(CO_3)_2^{2-}] \\ &= \frac{K_{104}[CO_3^{2-}]^4}{[OH^-]^4} + \frac{K_{105}[CO_3^{2-}]^5}{[OH^-]^4} + \frac{K_{122}[CO_3^{2-}]^2}{[OH^-]^2}\end{aligned} \tag{7}$$

The concentration of carbonate ($[CO_3^{2-}]$) was calculated from $[C]_{tot}$ and the dissociation constant of H_2CO_3(aq) and HCO_3^- ($pK_{a1} = 6.354$, $pK_{a2} = 10.329$ [9]), considering that $[C]_{tot}$ is much larger than $[Pu(IV)]_{tot}$. Due to their limited contribution under the investigated pH_c range and $[C]_{tot}$, the hydrolysis species of $Pu(OH)_m^{4-m}$ and the ternary Pu(IV) carbonate complex of $Pu(OH)_4(CO_3)_2^{4-}$ found at pH 12–13 [11] were not included in the equation.

The molar values of $I = (0.1, 0.5, 2.0$ and $5.0)$ mol·dm^{-3} were converted to the molal scale, $I_m = 0.1$, 0.5, 2.1, and 5.9 mol·kg^{-1}, based on the densities of $NaNO_3$ and the K_{1xy}

Table 1 Summary of the complex formation constants and solubility products in the Pu–carbonate systems ($I=0$)

Reactions		Values	Refs
$PuO_2(am,hyd)+2H_2O+4\,CO_3^{2-} \rightleftharpoons Pu(CO_3)_4^{4-}+4OH^-$	$\log_{10} K^{o}_{104}$	-21.33^a	[9]
$PuO_2(am,hyd)+2H_2O+5\,CO_3^{2-} \rightleftharpoons Pu(CO_3)_5^{6-}+4OH^-$	$\log_{10} K^{o}_{105}$	-22.68^a	[9]
	$\log_{10} K^{o}_{105}$	-22.67	[14]
$PuO_2(am,hyd)+2H_2O+2\,CO_3^{2-} \rightleftharpoons Pu(OH)_2(CO_3)_2^{2-}+2OH^-$	$\log_{10} K^{o}_{122}$	-12.09^a	[14]
	$\log_{10} K^{o}_{122}$	-10.73	[11]
$PuO_2(am,hyd)+2H_2O+3\,CO_3^{2-} \rightleftharpoons Pu(OH)_2(CO_3)_3^{4-}+2OH^-$	$\log_{10} K^{o}_{123}$	-12.0^b	Present study

[a]Used in the present analysis as fixed values

[b]Obtained by the SIT approach

for each ionic strength was calculated based on the specific ion interaction theory (SIT) approach [9].

$$\begin{aligned}\log_{10} K_{1xy} &= \log_{10} K^{\circ}_{1xy} - \log_{10}\gamma_{Pu(OH)_x(CO_3)_y^{4-x-2y}} - (4-x)\log_{10}\gamma_{OH^-} + y\log_{10}\gamma_{CO_3^{2-}} + 2\log_{10} a_w \\ &= \log_{10} K^{\circ}_{1xy} + \left\{(4-x-2y)^2 + (4-x) - 4y\right\}D \\ &\quad - \left\{\varepsilon\left(Pu(OH)_x(CO_3)_y^{4-x-2y}, Na^+\right) + (4-x)\varepsilon\left(OH^-, Na^+\right) - y\varepsilon\left(CO_3^{2-}, Na^+\right)\right\}\cdot I_m + 2\log_{10} a_w\end{aligned} \tag{8}$$

where K^{o}_{1xy} is the complex formation constant at $I_m=0$,$\varepsilon(Pu(OH)_x(CO_3)_y^{4-x-2y}, Na^+)$; $\varepsilon(OH^-, Na^+) = 0.04$ kg·mol^{-1} [9], and $\varepsilon(CO_3^{2-}, Na^+) = -0.08$ kg·mol^{-1} [9] represent the ion interaction coefficients for each species; and D and a_w are the Debye–Hückel term and activity of water at 25 °C. Since the ε values for $Pu(CO_3)_4^{4-}$, $Pu(CO_3)_5^{6-}$, and $Pu(OH)_2(CO_3)_2^{2-}$ have not been reported in the literature, they were assumed to be -0.2 kg·mol^{-1}, -0.3 kg·mol^{-1}, and -0.1 kg·mol^{-1}, respectively, according to the empirical correlation proposed by Hummel et al. [29].

Figure 5 shows the comparison of the experimental results and calculated Pu(IV) solubility as a sum of the concentrations of $Pu(CO_3)_4^{4-}$, $Pu(CO_3)_5^{6-}$, and $Pu(OH)_2(CO_3)_2^{2-}$. At $I=0.5$ mol·dm^{-3} in Fig. 5a and d, the experimental plots in the presence of constant $[C]_{tot}=0.16$ mol·dm^{-3} and constant pH_c 8.1–9.7 were well reproduced by the model, indicating that $Pu(OH)_2(CO_3)_2^{2-}$ is the main species. This agreed well with the results in [11, 14], where Pu(IV) solubility were measured at lower CO_3^{2-} concentration ($[CO_3^{2-}]<0.1$ mol·dm^{-3}). On the other hand, at $I=2.0$ mol·dm^{-3} in Figs. 5b, the calculated solubility underestimated the experimental results approximately by one order of magnitude in the region of pH_c 9–10. While the modeled equilibrium concentrations of all considered species, $Pu(CO_3)_4^{4-}$, $Pu(CO_3)_5^{6-}$, and $Pu(OH)_2(CO_3)_2^{2-}$, increase with I_m, this effect is not sufficient to explain the solubility data at $I=2.0$ mol·dm^{-3}. This indicates that an additional species is needed for a comprehensive thermodynamic model to reproduce the experimental results from low to high ionic strength.

3.2.2 Thermodynamic Model Containing $Pu(OH)_2(CO_3)_3^{3-}$

Schepperle and Yalcintas et al. performed batch solubility experiments with UO_2(am,hyd), NpO_2(am,hyd) and PuO_2(am,hyd) in the presence of 0.04 and 0.1 mol·dm^{-3} $[C]_{tot}$ at $8<pH_c<12.5$ in 0.1–5.0 mol·dm^{-3} NaCl solutions [15]. Based

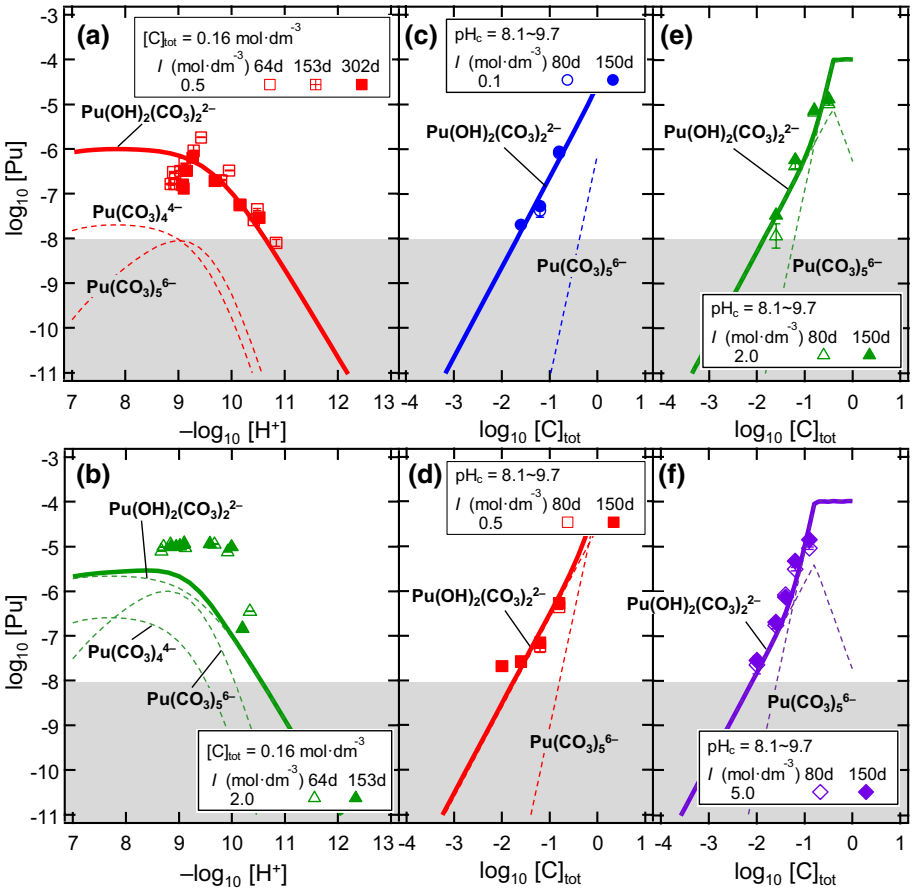

Fig. 5 Pu solubilities and calculated concentrations of $Pu(CO_3)_4^{4-}$, $Pu(CO_3)_5^{6-}$, and $Pu(OH)_2(CO_3)_2^{2-}$ based on the complex formation constants corrected by the SIT approach. The solution conditions are **a** in the presence of $[C]_{tot}$=0.16 mol·dm^{-3} at I=0.5 mol·dm^{-3}, **b** in the presence of $[C]_{tot}$=0.16 mol·dm^{-3} at I=2.0 mol·dm^{-3}, **c** at pH_c 8.1–9.7 at I=0.1 mol·dm^{-3}, **d** at pH_c 8.1–9.7 at I=0.5 mol·dm^{-3}, **e** at pH_c 8.1–9.7 at I=2.0 mol·dm^{-3}, and **f** at pH_c 8.1–9.7 at I=5.0 mol·dm^{-3}. The detection limit by the α-spectrometer is indicated by the gray field (Color figure online)

on the slope analysis and systematic evaluation of their solubility data, the authors suggested $An(OH)_2(CO_3)_3^{4-}$ as main An(IV) aqueous species, although its complex formation constant value for Pu(IV) was not reported in [15]. In the present study, therefore, we introduced $Pu(OH)_2(CO_3)_3^{4-}$ as an additional species to explain the experimental solubility data. In the analysis, the residual concentration ($[Pu]_{res}$) was first obtained by subtracting the calculated solubility as a sum of the concentrations of $Pu(CO_3)_4^{4-}$, $Pu(CO_3)_5^{6-}$, and $Pu(OH)_2(CO_3)_2^{2-}$ from the experimental values ($[Pu]_{tot}$). Then the $[Pu]_{res}$ as a function of pH_c and $[CO_3^{2-}]$ was fitted at each ionic strength to determine K_{123} value, as described below.

$$[\mathrm{PU}]_{\mathrm{res}} = [\mathrm{Pu}]_{\mathrm{tot}} - \left\{[\mathrm{Pu(CO_3)_4^{4-}}] + [\mathrm{Pu(CO_3)_5^{6-}}] + [\mathrm{Pu(OH)_2(CO_3)_2^{2-}}]\right\}$$
$$= [\mathrm{Pu(OH)_2(CO_3)_3^{4-}}] = \frac{K_{123}[\mathrm{CO_3^{2-}}]^3}{[\mathrm{OH^-}]^2} \quad (9)$$

3.2.2.1 SIT Approach As shown in Eq. 8, the complex formation constant of $\mathrm{Pu(OH)}_x(\mathrm{CO_3})_y^{4-x-2y}$ is expressed as a function of ionic strength (I_m) in mol·kg^{-1} (m) with the ion interaction coefficients for respective species. For each ionic strength from I_m = 0.1–5.9 mol·kg^{-1}, the concentrations of $\mathrm{Pu(CO_3)_4^{4-}}$, $\mathrm{Pu(CO_3)_5^{6-}}$, and $\mathrm{Pu(OH)_2(CO_3)_2^{2-}}$ were calculated from the reported constants and ion interaction coefficients (Tables 1, 2) as described above to obtain the $[\mathrm{Pu}]_{\mathrm{res}}$. The $\log_{10} K_{123}$ value was then determined by the least square fitting analysis of $[\mathrm{Pu}]_{\mathrm{res}}$ and plotted in Fig. 6a against the ionic strength.

$$\log_{10} K_{123} = \log_{10} K^\circ_{123} - \log_{10} \gamma_{\mathrm{Pu(OH)_2(CO_3)_3^{4-}}} - 2\log_{10}\gamma_{\mathrm{OH^-}} + 3\log_{10}\gamma_{\mathrm{CO_3^{2-}}} + 2\log_{10} a_\mathrm{w}$$
$$= \log_{10} K^\circ_{123} + 6D$$
$$-\left\{\varepsilon\left(\mathrm{Pu(OH)_2(CO_3)_3^{4-}},\mathrm{Na^+}\right) + 2\varepsilon\left(\mathrm{OH^-},\mathrm{Na^+}\right) - 3\varepsilon\left(\mathrm{CO_3^{2-}},\mathrm{Na^+}\right)\right\}\cdot I_\mathrm{m} + 2\log_{10} a_\mathrm{w} \quad (10)$$

Within the linear regression analysis of the $[\mathrm{Pu}]_{\mathrm{res}}$ values, $\varepsilon(\mathrm{Pu(OH)_2(CO_3)_3^{4-}}, \mathrm{Na^+})$ was fixed to −0.2 according to the empirical correction method [29]. Then, the $\log_{10} K^\mathrm{o}_{123} = -12.0$ was determined in the overall fitting of the $[\mathrm{Pu}]_{\mathrm{res}}$ values. The experimental $\log_{10} K_{123}$ values are scattered in Fig. 6a at I_m = 0.1 and 5.9 mol·kg^{-1}, where a lesser number of experimental data were obtained compared to those at I_m = 0.5 and 2.1 mol·kg^{-1}. The calculated solubility including $\mathrm{Pu(OH)_2(CO_3)_3^{4-}}$ are displayed in Fig. 7. The experimental values in the region of $\mathrm{pH_c}$ 9–10 at I = 2.0 mol·dm^{-3} were better reproduced by the contribution of $\mathrm{Pu(OH)_2(CO_3)_3^{4-}}$, while its contribution was not so prominent at I = 0.5 mol·dm^{-3}. The latter can be explained by the greater dependence of $\mathrm{Pu(OH)_2(CO_3)_3^{4-}}$ on ionic strength compared to $\mathrm{Pu(OH)_2(CO_3)_2^{2-}}$ arising from the more negative ε value and charge of $\mathrm{Pu(OH)_2(CO_3)_3^{4-}}$.

3.2.2.2 Pitzer Approach The activity model proposed by Pitzer [16, 17] has been widely used for the ionic strength correction in various systems including concentrated saline solu-

Table 2 SIT and Pitzer parameters used and determined in the present study

Species	SIT	Refs.	Pitzer			Refs.
	$\varepsilon(\mathrm{Na^+})$		$\beta^{(0)}$ ($\mathrm{Na^+}$)	$\beta^{(1)}$ ($\mathrm{Na^+}$)	C^ϕ ($\mathrm{Na^+}$)	
$\mathrm{NO_3^-}$	−0.04	[9]	0.0068	0.1783	−0.00072	[32]
$\mathrm{OH^-}$	0.04	[9]	0.0864	0.253	0.0044	[32]
$\mathrm{CO_3^{2-}}$	−0.08	[9]	0.0399	1.389	0.0044	[32]
$\mathrm{Pu(CO_3)_4^{4-}}$	−0.2[a]	Present study	–	–	–	
$\mathrm{Pu(CO_3)_5^{6-}}$	−0.3[a]		–	–	–	
$\mathrm{Pu(OH)_2(CO_3)_2^{2-}}$	−0.1[a]		–	–	–	
$\mathrm{Pu(OH)_2(CO_3)_3^{4-}}$	−0.2[a]		1.0118	9.4136	0	Present study

[a]Fixed in the analysis according to the empirical correction method[29]

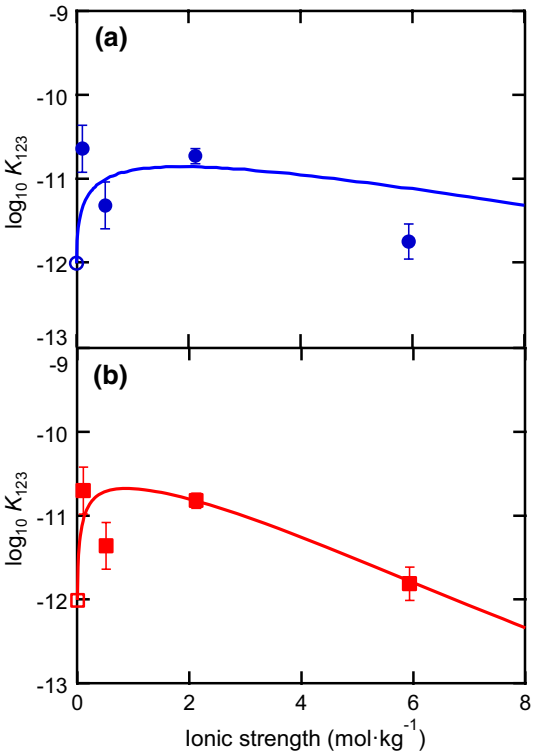

Fig. 6 Complex formation constant (K_{123}) of $Pu(OH)_2(CO_3)_3^{4-}$ as a function of ionic strength (I_m) with the ionic strength correction by **a** the SIT and **b** the Pitzer approaches. The filled symbols represent the experimental values determined by the least-square fitting analysis of $[Pu]_{res}$. The curves represent the calculated $\log_{10} K_{123}$ by the SIT and Pitzer approaches and the open symbols are the calculated values at $I_m = 0$

tions. In the present study, the Pitzer approach was applied to evaluate the complex formation constant and ion interaction parameters for the newly introduced $Pu(OH)_2(CO_3)_3^{4-}$ species. Due to lack of the reported Pitzer parameters for Pu(IV) carbonate species, the fitting analysis by the Pitzer approach was performed under the following constraints. The $[Pu]_{res}$ was obtained by subtracting the concentrations of $Pu(CO_3)_4^{4-}$, $Pu(CO_3)_5^{6-}$, and $Pu(OH)_2(CO_3)_2^{2-}$, which were calculated by SIT approach from the experimental solubility data of $[Pu]_{tot}$. The corresponding $\log_{10} K_{123}$ values shown in Fig. 6b determined from $[Pu]_{res}$ were then analyzed with the Pitzer formulations to determine the Pitzer parameters. Among the parameters, only the binary parameters $\beta^{(0)}$ and $\beta^{(1)}$ were treated as the fitting parameters and determined to be $\beta^{(0)} = 1.0118$ and $\beta^{(1)} = 9.4136$. Values for C^{ϕ}, $\beta^{(2)}$, and ternary ion interaction parameters were fixed at zero. The $\log_{10} K^{o}_{123}$ value of − 12.0 determined in the SIT approach was also treated as a fixed parameter. The used and determined parameters are summarized in Table 2 and the fitted curve by the Pitzer model are described in Fig. 6b. While the SIT approach has been sometimes limited to ionic strengths lower than approximately 3 $mol \cdot kg^{-1}$, the Pitzer approach is known to be applicable to higher ionic strength. Comparing both methods in Fig. 6, the Pitzer approach seems more able to reproduce the experimental values at $I_m = 5.9$ $mol \cdot kg^{-1}$. However, it is noteworthy that the calculated $\log_{10} K_{123}$ values by the SIT and Pitzer approaches at $I_m \leq 2.1$ $mol \cdot kg^{-1}$ are similar to each other and the Pu(IV) solubility in the presence of carbonate is well explained with both methods by taking $Pu(CO_3)_4^{4-}$, $Pu(CO_3)_5^{6-}$, $Pu(OH)_2(CO_3)_2^{2-}$ and $Pu(OH)_2(CO_3)_3^{4-}$ into account.

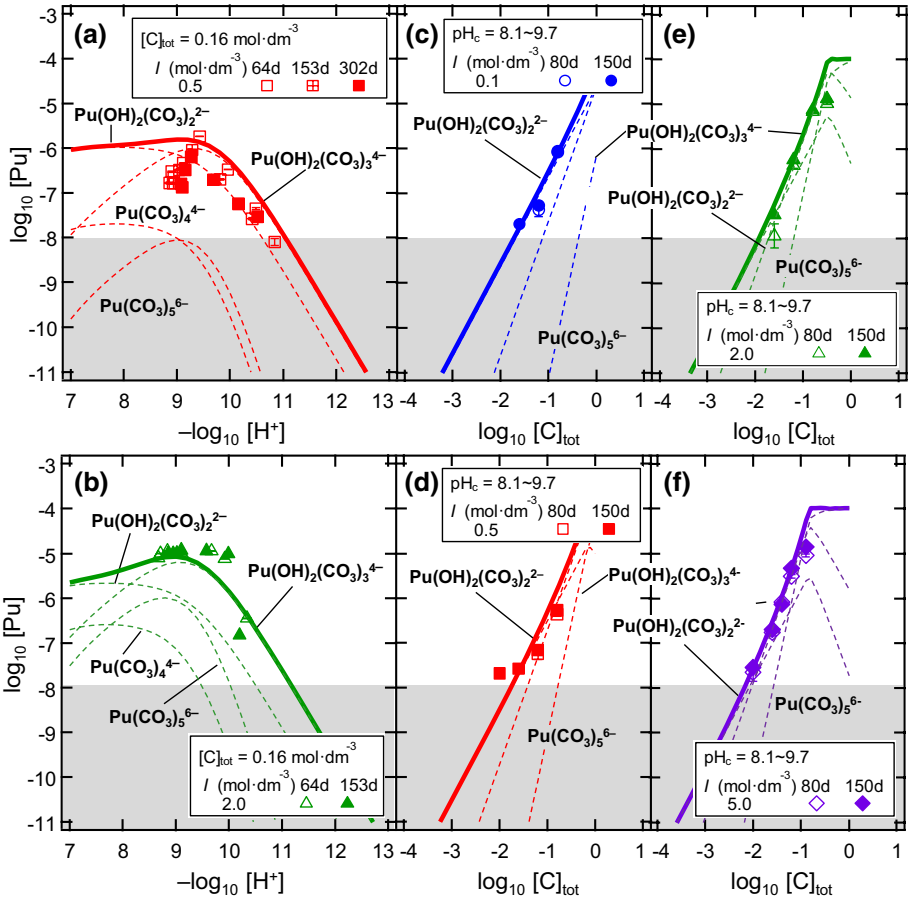

Fig. 7 Pu solubilities and calculated concentrations of $Pu(CO_3)_4^{4-}$, $Pu(CO_3)_5^{6-}$, $Pu(OH)_2(CO_3)_2^{2-}$, and $Pu(OH)_2(CO_3)_3^{4-}$ based on the complex formation constants corrected by the SIT approach. The solution conditions are **a** in the presence of $[C]_{tot}=0.16$ mol·dm^{-3} at $I=0.5$ mol·dm^{-3}, **b** in the presence of $[C]_{tot}=0.16$ mol·dm^{-3} at $I=2.0$ mol·dm^{-3}, **c** at pH_c 8.1–9.7 at $I=0.1$ mol·dm^{-3}, **d** at pH_c 8.1–9.7 at $I=0.5$ mol·dm^{-3}, **e** at pH_c 8.1–9.7 at $I=2.0$ mol·dm^{-3}, and **f** at pH_c 8.1–9.7 at $I=5.0$ mol·dm^{-3}. The detection limit by the α-spectrometer is indicated by the gray field (Color figure online)

4 Conclusions

The solubility of the plutonium amorphous hydrous oxide (PuO_2(am,hyd)) was investigated in the presence of carbonate ions under neutral to alkaline pH conditions in 0.1–5.0 mol·dm^{-3} $NaNO_3$ solutions. The observed dependence of Pu(IV) solubility on pH_c and $[CO_3^{2-}]$ in low to medium $NaNO_3$ concentrations agreed with previously reported data and was well reproduced by the thermodynamically calculated solubility curves, containing $Pu(CO_3)_4^{4-}$, $Pu(CO_3)_5^{6-}$, and $Pu(OH)_2(CO_3)_2^{2-}$. However, the Pu(IV) solubility in 2 mol·dm^{-3} $NaNO_3$ solutions was observed to be an order of magnitude higher than the calculated solubility curve as a sum of these species. The formation of $Pu(OH)_2(CO_3)_3^{4-}$ with the ionic strength correction by the specific ion interaction theory (SIT) and Pitzer

approaches was found to well reproduce the experimental results under low to high ionic strengths. The formation constant and the ionic strength correction parameters were determined in the analysis of the solubility data to establish a more comprehensive thermodynamic model.

Acknowledgements This study was partly conducted under the Visiting Researchers Program of the Institute for Integrated Radiation and Nuclear Science, Kyoto University (KURNS). The authors acknowledge Dr. Akihiro Uehara (currently National Institutes for Quantum and Radiological Science and Technology) and the facility staff at KURNS for their great contributions to the experiments.

Funding This work has been financially supported in part by a grant from the Ministry of Economy, Trade and Industry (METI).

Declarations

Conflict of interest There is no conflict of interests to declare.

References

1. Rai, D., Ryan, J.L.: Crystallinity and solubility of Pu(IV) oxide and hydrous oxide in aged aqueous suspensions. Radiochim. Acta **30**, 213–216 (1982)
2. Fujiwara, K., Yamana, H., Fujii, T., Moriyama, K.: Solubility product of plutonium hydrous oxide and its ionic strength dependence. Radiochim. Acta **90**, 857–861 (2002)
3. Haschke, J.M., Bassett, R.L.: Control of plutonium dioxide solubility by amorphous tetrahydroxide: a critical review of the model. Radiochim. Acta **90**, 505–509 (2002)
4. Rai, D., Gorby, Y.A., Fredrickson, J.K., Moore, D.A., Yui, M.: Reductive dissolution of PuO_2(am): the effect of Fe(II) and hydroquinone. J. Solution Chem. **31**, 433–453 (2002)
5. Neck, V., Altmaier, M., Seibert, A., Yun, J.I., Marquardt, C.M., Fanghänel, T.: Solubility and redox reactions of Pu(IV) hydrous oxide: evidence for the formation of PuO_{2+x}(s, hyd). Radiochim. Acta **95**, 193–207 (2007)
6. Ekberg, C., Larsson, K., Skarnemark, G., Ödegaard-Jensen, A., Persson, I.: The structure of plutonium(IV) oxide as hydrolysed clusters in aqueous suspensions. Dalton Trans. **42**, 2035–2040 (2013)
7. Lemire, R.J., Fuger, J., Spahiu, K., Nitsche, H., Ullman, W.J., Potter, P., Vitorge, P., Rand, M.H., Wanner, H., Rydberg, J.: Chemical thermodynamics of neptunium and plutonium. In: Brown, T.L., LeMay, H.E., Jr., Bursten, B.E. (eds.) Chemical Thermodynamics, vol. 4. Elsevier, Amsterdam (2003)
8. Neck, V., Kim, J.I.: Solubility and hydrolysis of tetravalent actinides. Radiochim. Acta **89**, 1–16 (2001)
9. Guillaumont, R., Fanghänel, T., Fuger, J., Grenthe, I., Neck, V., Palmer, D., Rand, M.: Update on the chemical thermodynamics of uranium, neptunium, plutonium, americium and technetium. In: Mompean, F.J., Illemassene, M., Domenech-Orti, B., Said, K. (eds.) Chemical Thermodynamics, vol. 5. Elsevier, Amsterdam (2003)
10. Moriyama, H., Sasaki, T., Kobayashi, T., Takagi, I.: Systematics of hydrolysis constants of tetravalent actinide ions. J. Nucl. Sci. Technol. **42**, 626–635 (2005)
11. Yamaguchi, T., Sakamoto, Y., Ohnuki, T.: Effect of the complexation on solubility of Pu(IV) in aqueous carbonate system. Radiochim. Acta **66**(67), 9–14 (1994)
12. Capdevila, H., Vitorge, P., Giffaut, E., Delmau, L.: Spectrophotometric study of the dissociation of the Pu(IV) carbonate limiting complex. Radiochim. Acta **74**, 93–98 (1996)
13. Clark, D.L., Conradson, S.D., Keogh, D.W., Palmer, P.D., Scott, B.L., Tait, C.D.: Identification of the limiting species in the plutonium(IV) carbonate system. Solid state and solution molecular structure of the $[Pu(CO_3)_5]^{6-}$ Ion. Inorg. Chem. **37**, 2893–2899 (1998)
14. Rai, D., Hess, N.J., Felmy, A.R., Moore, D.A., Yui, M., Vitorge, P.: A thermodynamic model for the solubility of PuO_2(am) in the aqueous K^+–HCO_3^-–CO_3^{2-}–OH^-–H_2O system. Radiochim. Acta **86**, 89–99 (1999)
15. Schepperle, J., Yalcintas, E., Fellhauer, D., Cevirim, N., Gaona, X., Altmaier, M., Geckeis, H.: Hydroxo-Carbonate Complex Formation and Solubility of Tetravalent Actinides at Alkaline pH

Conditions. 16th International Conference on the Chemistry and Migration Behaviour of Actinides and Fission Products in the Geosphere (MIGRATION 2017). Barcelona, Spain (2017)
16. Pitzer, KS., Mayorga, G.: Thermodynamics of electrolytes. II. Activity and osmotic coefficients for strong electrolytes with one or both ions univalent. J. Phys. Chem. **77**, 2300–2308 (1973)
17. Pitzer, KS.: Ion interaction approach: theory and data correlation. In: Pitzer, K.S. (ed.) Activity Coefficients in Electrolyte Solutions, 2nd edn. CRC Press, Boca Raton (1991)
18. Rai, D.: Solubility product of Pu(IV) hydrous oxide and equilibrium constants of Pu(IV)/Pu(V), Pu(IV)/Pu(VI) and Pu(V)/Pu(VI) couples. Radiochim. Acta **35**, 97–106 (1984)
19. André, L., Pauwels, H., Azaroual, M., Albrecht, A., Romero, M.-A.: Reactivity of nitrates in the different storage compartments of type-b wastes. In: Norris, S. (ed.) Clays in Natural & Engineered Barriers for Radioactive Waste Confinement. Geological Society, France (2007)
20. Japan Atomic Energy Agency: 2nd Progress Report on Research and Development for TRU Waste Disposal in Japan, JAEA-Review TRU-TR2-2007-01, JAEA, Tokai, Japan (2007)
21. Hicks, T., Baldwin, T.D., Hooker, P.J., Richardson, P., Chapman, N., McKinley, I., Neall, F.: Concepts for the Geological Disposal of Intermediate-Level Radioactive Waste. Galson Sciences Ltd., Rutland (2017)
22. Kienzler, B.: Schwach- und mittelradioaktive Abfälle: Organische Matrices. KIT Scientific Reports, Karlsruhe (2017)
23. Puigdomenech, I.: HYDRA (Hydrochemical Equilibrium-Constant Database) and MEDUSA (Make Equilibrium Diagrams Using Sophisticated Algorithms) Programs. Royal Institute of Technology, Sweden. http://www.ke-mi.kth.se/medusa
24. Altmaier, M., Gaona, X., Fellhauer, D., Clark, D.L., Runde, W.H., Hobart, D.E.: Aqueous solution and coordination chemistry of plutonium, plutonium handbook, Vol. 3. In: Clark, D., Geeson, D., Hanrahan, R. (eds.) Plutonium Handbook, 2nd edn. American Nuclear Society, La Grange Park (2019)
25. Baumann, A., Gaona, X., Yalçıntaş, E., Dardenne, K., Prüßmann, T., Rothe, J., Duckworth, S., Altmaier, M., Geckeis, H.: Impact of nitrate on the redox chemistry and solubility of Tc(IV) in alkaline, dilute to concentrated aqueous NaCl solutions. Appl. Geochem. **98**, 321–330 (2018)
26. Rai, D., Sterne, R.J., Moore, D.A.: Solubility of plutonium compounds and their behavior in soils. Soil Sci. Am. J. **44**, 490–495 (1980)
27. Fujiwara, K., Yamana, H., Fujii, T., Moriyama, H.: Solubility product of plutonium hydroxide. J. Nucl. Fuel Cycle Environ. **7**, 17–23 (2001)
28. Kobayashi, T., Sasaki, T.: Solubility of $Zr(OH)_4$(am) and the formation of Zr(IV) carbonate complexes in carbonate solutions containing 0.1–5.0 mol·dm^{-3} $NaNO_3$. J. Solution Chem. **46**, 1741–1759 (2017)
29. Hummel, W., Anderegg, G., Rao, L., Puigdomènech, I., Tochiyama, O.: Chemical thermodynamics of compounds and complexes of U, Np, Pu, Am, Tc, Se, Ni and Zr with selected organic ligands. In: Illemasséne, M., Perrone, J., Mompean, F.J. (eds.) Chemical Thermodynamics, vol. 9. Elsevier, Amsterdam (2005)
30. Rand, M., Fuger, J., Grenthe, I., Neck, V., Rai, D.: Chemical thermodynamics of thorium. In: Mompean, F.J., Perrone, J., Illemasséne, M. (eds.) Chemical Thermodynamics, vol. 11. Elsevier, Amsterdam (2009)
31. Delegard, C.H.: Effects of aging on $PuO_2{\cdot}xH_2O$ particle size in alkaline solution. Radiochim. Acta **101**, 313–322 (2013)
32. Meng, Z., Seinfeld, J.H., Saxena, P., Kim, Y.P.: Atmospheric gas–aerosol equilibrium: IV. Thermodynamics of carbonates. Aerosol Sci. Technol. **23**, 131–154 (1995)

Publisher's Note Springer Nature remains neutral with regard to jurisdictional claims in published maps and institutional affiliations.